Extract-gradient shape optimization of a 2D Euler flow

François Beux, Alain Dervieux

UNITÉ DE RECHERCHE
INRIA-SOPHIA ANTIPOLIS

Institut National
de Recherche
en Informatique
et en Automatique

Domaine de Voluceau
Rocquencourt
B.P.105
78153 Le Chesnay Cedex
France
Tél.:(1) 39 63 55 11

Rapports de Recherche

N° 1540

Programme 6
Calcul Scientifique, Modélisation et
Logiciel numérique par Ordinateur

EXACT-GRADIENT SHAPE OPTIMIZATION OF A 2D EULER FLOW

François BEUX
Alain DERVIEUX

Octobre 1991

RR-1540

EXACT-GRADIENT SHAPE OPTIMIZATION OF A 2 D EULER FLOW

OPTIMISATION DE PROFILS
PAR UNE METHODE DE GRADIENT EXACT
POUR UN ECOULEMENT 2 D EULERIEN

François BEUX **Alain DERVIEUX**

INRIA Sophia Antipolis
2004 Route des Lucioles 06360 VALBONNE
FRANCE

RESUME

Le problème de l'optimisation d'un obstacle plongé dans un écoulement régi par les équations d'Euler est étudié. On s'intéresse particulièrement, dans une perspective d'une méthode de gradient, à la différentiation de la solution de l'écoulement par rapport à la forme de l'obstacle. Dans le cas du problème continu, on définit formellement ces dérivées (formule de Hadamard) . Dans le cas discret, on choisit une méthode décentrée avec décomposition de flux différentiable et on montre la faisabilité du calcul du gradient par une méthode de l'adjoint sur une famille de problèmes. Le comportement des méthodes de gradient est décrit pour le cas d'un écoulement subsonique dans une tuyère.

ABSTRACT

The optimization of an obstacle shape put into an Euler flow is adressed. In order to apply a descent method, we consider the differentiation of the flow solution with respect to the shape. In the continuous case, we formally construct the derivatives (Hadamard variational formula). In the discrete case, we choose an upwind method with flux splitting, and we prove that an exact gradient can be computed using adjoint state. The behavior of a gradient method is studied for a family of nozzle flows.

Contents

1 Introduction

Calculating optimal aerodynamical shape is one among the oldest dreams of applied mathematicians and physicists, and many well known of them have contributed to the advancement of this question .
Many researchs were performed through " Calculus of variations " towards optimality conditions (see [1]) but it is clear that now the main point is to handle rather complicated flow models, that do not allow analytical derivations, but, instead, rather complex computer applications.
Also, many experiments have been performed, with models with increasing complexity, up to full potential flows (see [5] , [9]). The main difficulty is related to the important cost of one flow calculation; it's generally thought that a convenient class of model is the Reynolds-averaged Navier-Stokes equations, but in this case, a single calculation around a complete aircraft is more or less out of reach with today's computers. Moreover this cost must be multiplied by the points of design (several Mach regimes, ...) and the number of cost evaluations performed for optimization. Conversely choosing a simpler model is a delicate task if we want to be sure that the apparent improvement of the shape is not invalidated by the coarseness of the model. We propose in this paper to consider the Euler equations, a medium-complexity model that has not been much investigated.
We distinguish two approaches for optimization :
either (i) an exact gradient is computed or (ii) only the cost function is calculated (an approximate gradient is obtained by divided finite differences).
Exact gradient methods are more difficult to construct, programming by hand is quite complex, by they deliver n informations for one gradient (n : number of control variables) while methods of type (ii) give one information for one cost calculation (which, however, can be simplified by a perturbation approach). Another point is that exact gradient methods might be in the future more easily constructed thanks to automatical, Fortran writing, symbolic softwares.
In this paper we study an exact gradient approach; since the cost function is real valued, the chain rule through the state equation is expressed with the help of an adjoint state.
Some investigations of the adjoint state and Frechet derivatives with respect to shape are presented first for the continuous system in Section 2.
Then, in Section 3, the method applied for the discrete problem is described.
In the 4^{th} Section this is applied to a set of 2-D inverse problems.

2 Continuous problem

2.1 Hadamard's formula

Let Γ_{ad} be a set of parametrization included in $C^2([0,2\pi],I\!R^2)$; at any γ in Γ_{ad} , corresponds a regular subdomain Ω_γ of $I\!R^2$, the boundary at which is also denoted by γ .

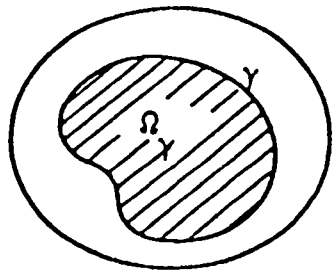

Figure 1:

We would find $W = (W_1, W_2, W_3, W_4) = (\rho, \rho u, \rho v, E) \in C^2(I\!R^2, I\!R^4)$ such that for all $\varphi = (\varphi_1, \varphi_2, \varphi_3, \varphi_4) \in (H^2(I\!R^2))^4$

$$\iint_{\Omega_\gamma} (F(W)\varphi_x + G(W)\varphi_y)dxdy - \int_\gamma \begin{pmatrix} 0 \\ P(W)n_x \\ P(W)n_y \\ 0 \end{pmatrix} \varphi d\sigma = 0 \qquad (1)$$

Where the boundary integral on γ stands for a slip condition;
$\vec{n} = (n_x, n_y)$ is the unitary outward normal vector on γ , P the boundary pressure, F and G the Euler's flux functions, given by :

For a perfect gas, $P = (\varpi - 1)\ (E - \frac{1}{2}\rho(u^2 + v^2))$ where $\varpi = \frac{c_p}{c_v}$ is the ratio of specific heats, and :

$$F(W) = \begin{pmatrix} \rho u \\ \rho u^2 + P \\ \rho uv \\ (E+P)u \end{pmatrix} \quad G(W) = \begin{pmatrix} \rho v \\ \rho uv \\ \rho v^2 + P \\ (E+P)v \end{pmatrix} \quad ;$$

where we use the following notations :
ρ is the density, u and v are the horizontal and vertical velocity components and E is the total energy per unit volume.

We assume the existence of a differentiable application $\bar{W} : \Gamma_{ad} \rightarrow C^2(I\!R^2, I\!R^4)$ *such that:*

$$\forall\, \gamma \in \Gamma_{ad} \quad \bar{W}(\gamma)|_{\Omega_\gamma} = W \ \textit{solution of} \ (1)$$

We refer to Annex 1 for a simplified model for which the above statement is rigorously established.

Then we define :

$$\Psi : \Gamma_{ad} \times C^2(I\!R^2, I\!R^4) \rightarrow ((H^2(I\!R^2))^4)'$$

With :

$$\forall \gamma \in \Gamma_{ad} \qquad \Psi(\gamma, \bar{W}(\gamma)) = 0$$

We obtain after differentiation :

$$\frac{\partial \Psi}{\partial \gamma}\delta\gamma + \frac{\partial \Psi}{\partial W}\frac{d\bar{W}}{d\gamma}\delta\gamma = 0 \tag{2}$$

If we write explicitly the different terms, we get :

$$< \frac{\partial \Psi}{\partial W}\frac{d\bar{W}}{d\gamma}\delta\gamma, \varphi > = \iint_{\Omega_\gamma} \frac{\partial F}{\partial W}\frac{d\bar{W}}{d\gamma}\delta\gamma\ \varphi_x\ dxdy + \iint_{\Omega_\gamma} \frac{\partial G}{\partial W}\frac{d\bar{W}}{d\gamma}\delta\gamma\ \varphi_y\ dxdy$$

$$- \int_\gamma \begin{pmatrix} 0 \\ n_x \dfrac{\partial P}{\partial W}\dfrac{d\bar{W}}{d\gamma}\delta\gamma \\ n_y \dfrac{\partial P}{\partial W}\dfrac{d\bar{W}}{d\gamma}\delta\gamma \\ 0 \end{pmatrix} \varphi\, d\sigma \tag{3}$$

But it's more delicate to differentiate with respect to integral limits, we must use some " Continuum Mechanics lemmas " recalled in Annex 2, and introduce a vector field describing the change of boundary :

Let $\vec{V}$ a regular vector field on $I\!R^2$; the boundary "$\gamma + \delta\gamma$" is obtained by convention as the set of points M : $M = \{N + \vec{V}(N) . \delta\gamma , N \epsilon \gamma\}$.

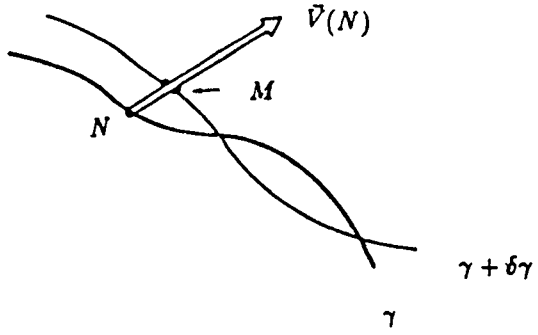

Figure 2: boundary parametrization

Let us write $\Psi(\gamma, \bar{W}(\gamma)$ under the form : $\iint_{\Omega_\gamma} C(\gamma)\, dxdy$;
using Stokes formula we have:

$$\int_\gamma P n_x \varphi_2 d\sigma = \int_\gamma \begin{pmatrix} P\varphi_2 \\ 0 \end{pmatrix} \vec{n} d\sigma = \iint_{\Omega_\gamma} div \begin{pmatrix} \bar{P}\varphi_2 \\ 0 \end{pmatrix} dxdy = \iint_{\Omega_\gamma} (\frac{\partial \bar{P}}{\partial x}\varphi_2 + \bar{P}\frac{\partial \varphi_2}{\partial x})dxdy$$

Where $\bar{P}$ is any extension of P on Ω_γ

In the same way :

$$\int_\gamma P n_y\, \varphi_3\, d\sigma = \iint_{\Omega_\gamma} (\frac{\partial \bar{P}}{\partial y}\varphi_3 + \bar{P}\frac{\partial \varphi_3}{\partial y})dxdy \ .$$

Then :

$$< \frac{\partial \Psi}{\partial \gamma}\delta\gamma, \varphi >= \frac{d}{d\gamma}\iint_{\Omega_\gamma} [\, F(W)\varphi_x + G(W)\varphi_y - \begin{pmatrix} 0 \\ \frac{\partial P}{\partial x} \\ \frac{\partial P}{\partial y} \\ 0 \end{pmatrix} \varphi - \bar{P} \begin{pmatrix} 0 \\ \frac{\partial \varphi_2}{\partial x} \\ \frac{\partial \varphi_3}{\partial y} \\ 0 \end{pmatrix}]\, dxdy\, \delta\gamma$$

And using " Continuum Mechanics Lemma 1 ", we obtain :

$$< \frac{\partial \Psi}{\partial \gamma} \delta\gamma, \varphi > = \int_\gamma (F(W)\,\varphi_x + G(W)\,\varphi_y) < \vec{n}, \vec{V} > \delta\gamma\, d\sigma$$

$$- \int_\gamma \left(\begin{pmatrix} 0 \\ \frac{\partial P}{\partial x} \\ \frac{\partial P}{\partial y} \\ 0 \end{pmatrix} \varphi - P \begin{pmatrix} 0 \\ \frac{\partial \varphi_2}{\partial x} \\ \frac{\partial \varphi_3}{\partial y} \\ 0 \end{pmatrix} \right) < \vec{n}, \vec{V} > \delta\gamma\, d\sigma \qquad (4)$$

Finally, the variations of the flow variables when the shape is changed are described by the following system :

$$\iint_{\Omega_\gamma} \frac{\partial F}{\partial W} \frac{d\bar{W}}{d\gamma} \delta\gamma\, \varphi_x\, dxdy + \iint_{\Omega_\gamma} \frac{\partial G}{\partial W} \frac{d\bar{W}}{d\gamma} \delta\gamma\, \varphi_y\, dxdy =$$

$$\int_\gamma \begin{pmatrix} 0 \\ \frac{\partial P}{\partial W} n_x \\ \frac{\partial P}{\partial W} n_y \\ 0 \end{pmatrix} \frac{d\bar{W}}{d\gamma} \delta\gamma\, \varphi\, d\sigma - \int_\gamma (F(W)\,\varphi_x + G(W)\,\varphi_y) < \vec{n}, \vec{V} > \delta\gamma\, d\sigma \qquad (5)$$

$$+ \int_\gamma \left(\begin{pmatrix} 0 \\ \frac{\partial P}{\partial x} \\ \frac{\partial P}{\partial y} \\ 0 \end{pmatrix} \varphi - P \begin{pmatrix} 0 \\ \frac{\partial \varphi_2}{\partial x} \\ \frac{\partial \varphi_3}{\partial y} \\ 0 \end{pmatrix} \right) < \vec{n}, \vec{V} > \delta\gamma\, d\sigma$$

With $\dfrac{\partial P}{\partial W} = (\varpi - 1)(u^2 + v^2, -u, -v, 1)$;

$\dfrac{\partial F}{\partial W}$, $\dfrac{\partial G}{\partial W}$ are diagonalisable and their eigenvalues are : $(\,u\,,\,u\,,\,u + c\,,\,u - c\,)$.

2.2 Gradient of a functional

We define two functionals $J : \Gamma_{ad} \times C^2(I\!R^2, I\!R^4) \rightarrow I\!R$ and $j : \Gamma_{ad} \rightarrow I\!R$ such that

$$\forall \gamma \in \Gamma_{ad} \quad j(\gamma) = J(\gamma, \bar{W}(\gamma))$$

Let $\delta\gamma$ an element of Γ_{ad} , we have :

$$\frac{dj}{d\gamma}(\gamma)\,\delta\gamma = \frac{\partial J}{\partial \gamma}(\gamma, W)\,\delta\gamma + < \frac{\partial J}{\partial W}(\gamma, W)\,,\frac{d\bar{W}}{d\gamma}(\gamma)\,\delta\gamma >$$

Where $< , >$ represents the duality between $(C^2(I\!R^2, I\!R^4))'$ and $C^2(I\!R^2, I\!R^4)$.
Using the differentiation of $\Psi(\gamma, \bar{W}(\gamma))$ we get :

$$\frac{dj}{d\gamma}(\gamma)\,\delta\gamma = \frac{\partial J}{\partial \gamma}(\gamma, W)\,\delta\gamma - < \frac{\partial J}{\partial W}(\gamma, W)\,,(\frac{\partial \Psi}{\partial W}(\gamma, w))^{-1}\frac{\partial \Psi}{\partial \gamma}(\gamma, W)\,\delta\gamma >$$

or :

$$\frac{dj}{d\gamma}(\gamma)\,\delta\gamma = \frac{\partial J}{\partial \gamma}(\gamma, W)\,\delta\gamma - < ((\frac{\partial \Psi}{\partial W}(\gamma, W))^{-1})^{*}\frac{\partial J}{\partial W}(\gamma, W)\,,\frac{\partial \Psi}{\partial \gamma}(\gamma, W)\,\delta\gamma >$$

where the star holds for the adjoint operator; so in conclusion :

$$\frac{dj}{d\gamma}(\gamma)\,\delta\gamma = \frac{\partial J}{\partial \gamma}(\gamma, W)\delta\gamma - < \Pi, \frac{\partial \Psi}{\partial \gamma}(\gamma, W)\,\delta\gamma > \ , \tag{6}$$

$$\text{with} \quad (\frac{\partial \Psi}{\partial \mathrm{W}}(\gamma, \mathrm{W}))^{*}\Pi = \frac{\partial \mathrm{J}}{\partial \mathrm{W}}(\gamma, \mathrm{W}) \tag{7}$$

2.3 An example

Let us consider the following functional :

$$\forall \gamma \in \Gamma_{ad}\ , \quad j(\gamma) = \frac{1}{2} \parallel z(\gamma) - z_d \parallel^2_{L^2(\Omega_0)}$$

Where $z(\gamma)$ is a solution of (1) , and $z_d \in L^2(\Omega_0)$, with Ω_0 equal to a fixed open set such that $\forall \gamma \in \Gamma_{ad}\ \bar{\Omega}_0 \subset \Omega_\gamma$.
In order to obtain the adjoint state for this particular functional, we shall develop the equation (7) .
Let φ an element of $\mathcal{C}^2(I\!R^2, I\!R^4)$, we have :

$$< (\frac{\partial \Psi}{\partial W}(\gamma, z)\ )^* \Pi, \varphi > = < \Pi, \frac{\partial \Psi}{\partial W}(\gamma, z)\ \varphi >$$

$\Pi \in ((H^2(I\!R^2))^4)'$, which is isomorph to $(H^2(I\!R^2))^4$; to Π corresponds an element π of $(H^2(I\!R^2))^4$.
Then the adjoint state equation can be written as :

$$< \frac{\partial \Psi}{\partial W}(\gamma, z)\ \varphi\ ,\ \pi > = < \frac{\partial J}{\partial W}(\gamma, z)\ ,\ \varphi >$$

Where:

$$< \frac{\partial J}{\partial W}(\gamma, z)\ ,\ \varphi > = \int\int_{\Omega_0} (z(\gamma) - z_d)\ .\ \varphi\ dx dy$$

So, if we note the scalar product of $I\!R^4$ by $\ll\ ,\ \gg$, we have for all $\varphi \in \mathcal{C}^2(I\!R^2, I\!R^4)$:

$$\int\int_{\Omega_\gamma} \ll \frac{\partial F}{\partial W} \varphi, \pi_x \gg + \ll \frac{\partial G}{\partial W}\ \varphi\ ,\ \pi_y \gg\ dx\ dy\ =$$

$$\int\int_{\Omega_0} \ll z(\gamma) - z_d\ ,\ \varphi \gg\ dx\ dy\ + \int_{\partial\Omega_\gamma} \ll \begin{pmatrix} 0 \\ n_x \frac{\partial P}{\partial W}\ .\ \varphi \\ n_y \frac{\partial P}{\partial W}\ .\ \varphi \\ 0 \end{pmatrix}\ ,\ \pi\ \gg\ d\sigma \qquad (8)$$

Let φ such that $\varphi|_{\partial\Omega_\gamma} = 0$, we obtain :

$$\int\int_{\Omega_\gamma} \ll \varphi\ ,\ (\frac{\partial F}{\partial W})^* \pi_x + (\frac{\partial G}{\partial W})^* \pi_y \gg\ dx\ dy\ - \int\int_{\Omega_0} \ll z(\gamma) - z_d\ ,\ \varphi \gg\ dx\ dy = 0$$

Since this relation is verified by all test functions equals to zero on $\partial\Omega_\gamma$, we have:

$$(\frac{\partial F}{\partial W})^* \pi_x + (\frac{\partial G}{\partial W})^* \pi_y = \chi_{\Omega_0}(z(\gamma) - z_d) \quad \text{in } \Omega_\gamma$$

So if we return to the equation (8), only the term of the boundary integral appears, that we can write as:

$$\int_{\partial\Omega_\gamma} \ll \mathcal{A}\varphi \, , \, \pi \gg d\sigma = 0 \qquad \text{with} \quad \mathcal{A} = \begin{pmatrix} 0 & 0 & 0 & 0 \\ n_x \frac{\partial P}{\partial W_1} & n_x \frac{\partial P}{\partial W_2} & n_x \frac{\partial P}{\partial W_3} & n_x \frac{\partial P}{\partial W_4} \\ n_y \frac{\partial P}{\partial W_1} & n_y \frac{\partial P}{\partial W_2} & n_y \frac{\partial P}{\partial W_3} & n_y \frac{\partial P}{\partial W_4} \\ 0 & 0 & 0 & 0 \end{pmatrix}$$

Using the adjoint of $\mathcal{A}$:

$$\int_{\partial\Omega_\gamma} \ll \varphi \, , \, \mathcal{A}^*\pi \gg d\sigma = \int_{\partial\Omega_\gamma} \ll \varphi \, , \, (n_x\pi_2 + n_y\pi_3)\frac{\partial P}{\partial W} \gg d\sigma = 0$$

Therefore $(n_x\pi_2 + n_y\pi_3)\frac{\partial P}{\partial W} = \vec{0}$, and since $\frac{\partial P}{\partial W_4} = \varpi - 1$ is constant, independent of P , we obtain finally on $\partial\Omega_\gamma$ the following slip condition :

$$n_x\pi_2 + n_y\pi_3 = 0$$

In conclusion, for this problem we have the following adjoint system :

$$\begin{cases} \pi(\gamma) \in H^2(I\!R^2))^4 \\ (\frac{\partial F}{\partial W})^* \pi_x + (\frac{\partial G}{\partial W})^* \pi_y = \chi_{\Omega_0}(z(\gamma) - z_d) \quad \text{in } \Omega_\gamma \\ \begin{pmatrix} \pi_2 \\ \pi_3 \end{pmatrix} . \vec{n} = 0 \quad \text{on } \partial\Omega_\gamma \end{cases} \tag{9}$$

Where χ_{Ω_0} is the characteristic function of Ω_0.

Under the differentiability assumptions of Section 2.1 , the Gateaux-derivative of j at γ_0 and in the θ direction is given by :

$$j'(\gamma_0,\theta) = -\int_{\partial\Omega_{\gamma_0}} (F(W)\,\pi_x + G(W)\,\pi_y) < \vec{n},\vec{V} > \theta\, d\sigma$$

$$+\int_{\partial\Omega_{\gamma_0}} \left(\begin{pmatrix} 0 \\ \frac{\partial P}{\partial x} \\ \frac{\partial P}{\partial y} \\ 0 \end{pmatrix} \pi - P \begin{pmatrix} 0 \\ \frac{\partial \pi_2}{\partial x} \\ \frac{\partial \pi_3}{\partial y} \\ 0 \end{pmatrix} \right) < \vec{n},\vec{V} > \theta\, d\sigma \qquad (10)$$

3 Discrete problem

3.1 Geometrical data

We consider a nozzle having the following characteristics :
x varies between $-2.$ and $4.$, it is convergent-divergent with symmetry with respect to $x = 1.$
The bottom shape is a straight segment .
Height is 0.5 for x in $[\,-2.\,,\,0.\,] \cup [\,2.\,,\,4.\,]$, and on the part to optimize, i.e for x in $[\,0.\,,\,2.\,]$, height is a variable curve (see Figure 3).

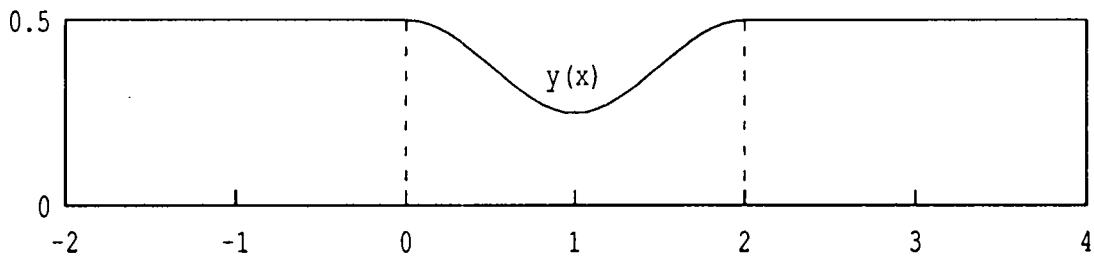

Figure 3: sketch of the computational domain

We have a triangular mesh where the abscissae are fixed and the ordinates change only for x in $[\,0.\,,\,2.\,]$.
We use then a "concertina like" mesh, i.e :
Let m the number of points in ordinates; if we note $y_i(x)$ the ordinate of the i^{th} mesh node which has x for abscissa, we have the relation :
For all i in $[\,1\,,\,\ldots\,,\,\mathrm{m}]$, $y_i(x) = \dfrac{y_i(0)}{y_m(0)}\, y_m(x)$
So the position of each node depends simply on $\{\, y_m(x) \,/\, x \in [\,0.\,,\,2.\,] \,\}$.
(We give in Figure 18 and 19 two examples of this type of mesh).

3.2 Numerical approximation for Euler's equations

We use a triangular upwind finite volume formulation , for each vertex i we have:

$$\Psi_{Euler}(W^n) = \sum_{j \in \kappa(i)} \Phi(W_{ij}^n, W_{ji}^n, \int_{\partial C_{ij}} \vec{n}\, d\sigma) \;+\; \text{Boundary conditions}$$

Where $\kappa(i)$ is the set of neightboring nodes of i, ∂C_{ij} the intersection between cell' s boundary of i and j, $\vec{n}$ the outward normal vector on ∂C_i, Ψ a numerical flux function . We choose for Ψ the Van Leer flux function which is differentiable.

Therefore for solving the discrete system for the Euler steady equations, we use an implicit linearized time advancing iteration :

$$(\frac{I}{\Delta t} + \Psi'(W^n))\delta W^{n+1} = \Psi(W^n) \tag{11}$$

(We recall that when Δt is arbitrarily large, this is like a Newton method).
Where $\Psi'(W^n)$ is computed without approximation.

3.3 Gradient's computation

The parameters of optimization are the ordinates at some boundary nodes, $\gamma = (\gamma_1, ..., \gamma_l)$. We construct a "concertina like" mesh, in such a way that the mesh's deformation is an ordinate change and depends only on the control γ.
Let $j : I\!R^l \rightarrow I\!R$ the cost functional, and $J : I\!R^l \times I\!R^{4m} \rightarrow I\!R$, where l is the control parameters number and m the nodes number of the mesh. We have :

$$j(\gamma) = J(\gamma, W(\gamma)) \quad \forall \gamma \in I\!R^l$$

Computing a Frechet derivative with respect to the shape, as in the continuous approach , we obtain here :

$$\forall \delta\gamma \in I\!R^l \quad < \frac{\partial j}{\partial \gamma}, \delta\gamma > = < \frac{\partial J}{\partial \gamma}, \delta\gamma > - < \Pi, \frac{\partial \Psi}{\partial \gamma}\delta\gamma >$$

With Π , the adjoint state, defined by $(\frac{\partial \Psi}{\partial W})^* \Pi = \frac{\partial J}{\partial W}$

Where $< , >$ is a scalar product, $\frac{\partial j}{\partial \gamma}$, $\frac{\partial J}{\partial \gamma}$ are vectors of $I\!R^l$, $\frac{\partial J}{\partial W}$, Π a vector of $I\!R^{4m}$, $\frac{\partial \Psi}{\partial \gamma}$ a matrix of $M_{4m,l}(I\!R)$ and $\frac{\partial \Psi}{\partial W}$ a matrix of $M_{4m,4m}(I\!R)$.
$\frac{\partial \Psi}{\partial \gamma}$ has been computed at the same time as the flux Ψ, i.e. when we compute $W(\gamma)$. We have now to look at the computation of the others terms.

Cost functional and its derivatives
To resolve an inverse problem we define j by : $j = \int_\Gamma (P - P^d)^2 d\sigma$ where P^d is the desired pressure

$$j = \sum_i \int_{\Gamma_i} (P - P^d)^2 d\sigma = \sum_i \int_{x_i}^{x_{i+1}} (P - P^d)^2 [1 + (\frac{\Delta y_i}{\Delta x_i})^2]^{\frac{1}{2}} dx$$

Using trapezoidal formula we obtain :

$$j = \frac{1}{2} \sum_i \| \vec{\eta_i} \| ((P_{i+1} - P^d_{i+1})^2 + (P_i - P^d_i)^2)$$

Where $\vec{\eta_i}$, the normal vector on Γ_i, is the only variable which depends explicitly of γ so :

$$\frac{\partial J}{\partial \gamma_k} = \frac{1}{2}\sum_{i=0}^{l}((P_{i+1} - P_{i+1}^d)^2 + (P_i - P_i^d)^2)\frac{\partial \parallel \vec{\eta_i} \parallel}{\partial \gamma_k}$$

If we notice that : $G_i = \frac{1}{2}((P_{i+1} - P_{i+1}^d)^2 + (P_i - P_i^d)^2)\frac{(y_{i+1} - y_i)}{\parallel \vec{\eta_i} \parallel}$

we have finally $\frac{\partial J}{\partial \gamma_k} = G_{k-1} - G_k$.

To differentiate with respect to geometry variables, we split J in the following way :

$$J = \frac{1}{2}\sum_{i=1}^{n} \parallel \vec{\eta_i} \parallel (P_i - P_i^d)^2 + \frac{1}{2}\sum_{i=2}^{n+1} \parallel \vec{\eta_i} - 1 \parallel (P_i - P_i^d)^2$$

Let $a_0 = a_{n+1} = 0$ and $a_i = \parallel \vec{\eta_i} \parallel$ for $i = 1, ..., n$, we can write then :

$$J = \frac{1}{2}\sum_{i=1}^{n+1}(a_i + a_{i-1})(P_i - P_i^d)^2$$

And finally after derivation :

$$\frac{\partial J}{\partial W} = \sum_{i=1}^{n+1}(a_i + a_{i-1})(P_i - P_i^d)\frac{\partial P_i}{\partial W_k}$$

Adjoint state

To obtain the adjoint state, we have to solve a linear system :

$$A_n \Pi = \frac{\partial J}{\partial W} \qquad with \quad A_n = (\Psi'(W^n))^t$$

Where A_n , a matrix of $M_{4m,4m}(I\!R)$, seems to be very costly.
But $\Psi'(W^n)$ has been already computed in our Euler equations resolution , when we use the unsteady implicit linearized time stepping (see in Section 3.2)
So A_n can be deduced directly from equation 11 without any additional calculation.

Optimization chart

We present now a sketch of the gradient calculation and the optimization algorithm, first for a simple gradient (Figure 4) and next for a conjugate gradient with an one-dimensional minimization (Figure 5).

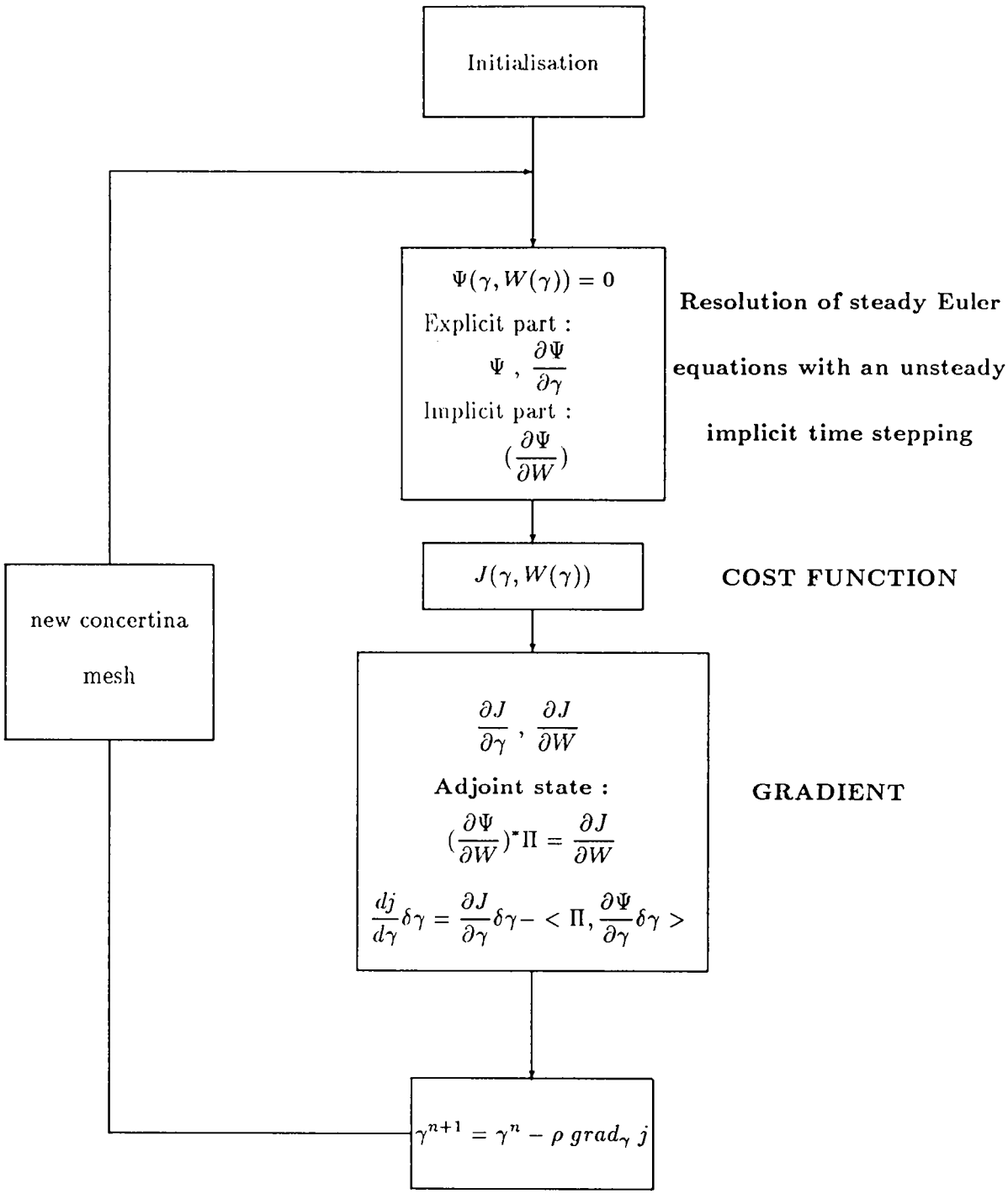

Figure 4: Simple gradient

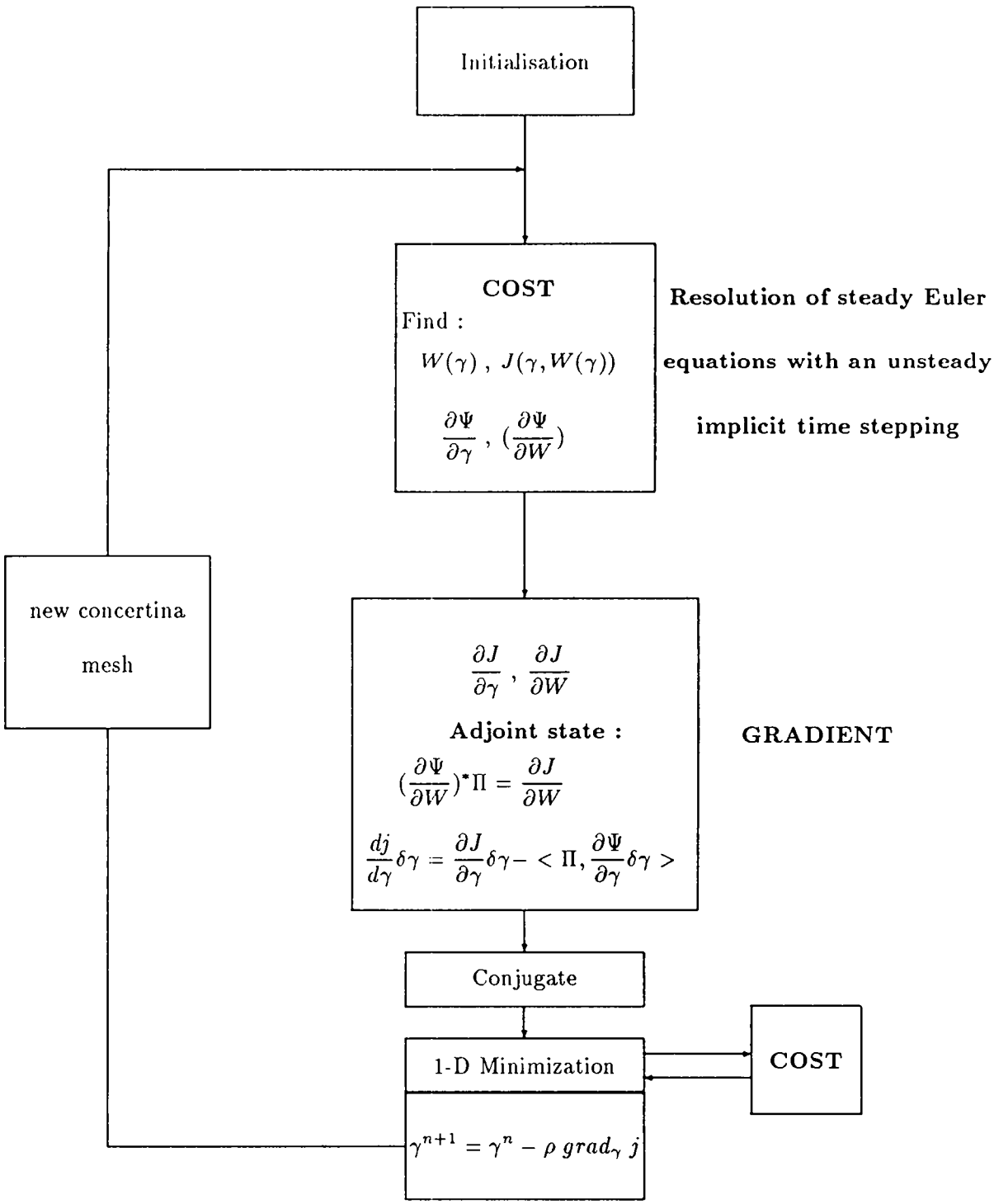

Figure 5: Conjugate gradient

4 Numerical experiments

We present a set of academical experiments referred as " inverse problem solutions ".

In all these numerical experiments the flow is subsonic with a farfield mach number equal to .2 .
In the sequel the exact gradient is used inside a Polak-Ribière conjugate gradient in which an one-dimensional minimization is performed by dichotomy, completed by a final parabolic interpolation; generally, a conjugate gradient iteration calls about 5 times the cost function.
(We present in Figure 17 a comparison between simple and conjugate gradient convergence for the test case 3).

4.1 Experiment chart

In a so-called "inverse problem solution", an ideal geometry γ_d is first choosen and the discrete flow is computed to construct the cost functional so that for γ_d, the cost is minimum and equal to zero.
Then an initial geometry (different from the ideal one) is choosen and optimization is started from this initial geometry with the above cost function. The purpose is to measure the ability of the minimization algorithm to find the ideal geometry.

4.2 Validation : comparison with divided differences

To validate the exact gradient computation, we compare it with an approximate gradient; indeed the divided finite differences $\frac{j(\gamma+\delta\gamma)-j(\gamma)}{\|\delta\gamma\|}$ approach the G-derivative of j with respect to γ when the shape perturbation $\delta\gamma$ is small enough .
Let e_k be the k^{th} canonical base vector of $I\!R^l$, and ε a real number, then εe_k represents a perturbation of the k^{th} control parameter .
So for each $k \in [1,..,l]$ and for different values of ε we compute $\delta_1^k = \frac{\partial j}{\partial \gamma_k}$ and $\delta_2^k = \frac{j(\gamma+\varepsilon e_k)-j(\gamma)}{\varepsilon}$.

We consider the same configuration as in test case 1 (see Section 4.3) where the direct and adjoint systems are always solved up to the machine double precision accuracy. And also we achieve a complete convergence of the Euler equations and a good resolution of the differents linear systems (i.e. with a lot of iterations of Jacobi). The results are presented, for six different values of k $(k = 1,3,6,9,12,16)$, in Figure 6 in which is sketched $Log(\frac{\delta_2^k-\delta_1^k}{\delta_1^k})$ as a function of $Log(\varepsilon)$:

$Log(\frac{\delta_2^k - \delta_1^k}{\delta_1^k})$

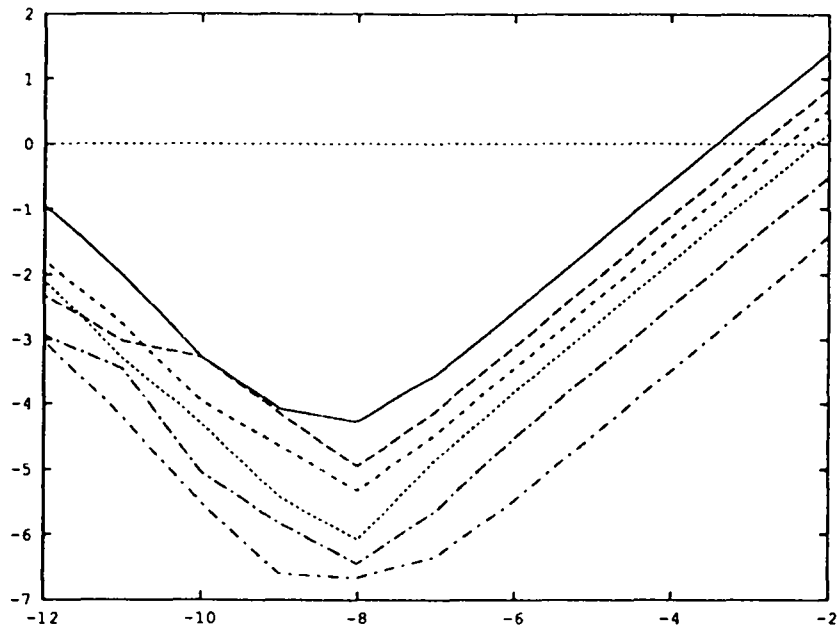

Figure 6: Accuracy of divised difference for different components of the control variable

We observe a good accordance between δ_1^k and δ_2^k ($\frac{\delta_2^k - \delta_1^k}{\delta_1^k}$ depends linearly on ε) except when ε is too small, because of round-off errors .
So we can deduce that to use correctly the divided differences we have to choose a good value of ε , neither too small nor too large .

4.3 Sensitivity to shape

We consider the two following shapes :

$$\gamma_1 \ : \qquad y(x) = \frac{19}{40} + \frac{1}{40}\sin(\pi(x + \frac{1}{2}))$$

The corresponding flow for γ_1 is presented (Mach contours) in Figure 7 for a mesh of 423 nodes (31 control parameters)

$$\gamma_2 \ : \quad \begin{cases} For \ \ 0 \le x \le \frac{1}{2} \quad y(x) = \frac{9}{16} - \frac{1}{16}\cos(2\pi x) \\ For \ \ \frac{1}{2} \le x \le 1 \quad y(x) = 6x^3 - \frac{27}{2}x^2 + 9x - \frac{5}{4} \\ For \ \ 1 \le x \le 2 \quad y(x) = y(2 - x) \end{cases}$$

The flow for γ_2 is presented in Figure 8 (for also a 423-node mesh).

Test case 1 :

In a first experiment, the functional has shape γ_1 as optimum and the initial shape is choosen equal to γ_2 .
Then a good convergence to the above optimum is observed in both cost magnitude (reduced by 10 orders of magnitude after 260 conjugate gradient steps) and in gradient norm (reduced by about 6 orders of magnitude at the same time); the corresponding shapes are given in Figure 9 .

Test case 2 :
If, conversely, γ_2 is the optimum and γ_1 the initial shape, the convergence is slowening after about 40 iterations and the problem becomes very stiff, hardly moving from a configuration (Figure 10) that is not a local minimum, as is observed from the gradient norm behaviour.
But, if now we increase the accuracy for the resolution of direct and adjoint linear system (in fact we do five times more Jacobi relaxations) we obtain a good convergence represented in Figure 12. The corresponding shapes of both cases are given respectively in Figure 11 and in Figure 13.

4.4 Sensitivity to mesh size

For this study, we choose a test case of medium stiffness, intermediate between test case 1 and test case 2 :

Test case 3 :
With the same 423-nodes mesh family, we consider the following optimum shape :

$$\gamma_3 : \qquad y(x) = \frac{3}{8} + \frac{1}{8} sin(\pi(x + \frac{1}{2}))$$

For this case the amplitude is 5 times larger than for γ_1 but now we start from the following constant shape :

$$\gamma_4 : \qquad y(x) = \frac{1}{2}$$

We observe from the convergence curves of both cost (Figure 14) and gradient (Figure 15) some stiffness: in fact, between iteration 20 and 80, convergence is much slower; then we get a new acceleration that, on our opinion, is provided by conjugaison of the descent directions.
Finally, a convergence of 8 orders of magnitude for cost (4 for gradient) is obtained after 260 conjugate-gradient iterations; we give in Figure 16 a set of five caracteristic iterate shapes.

Test case 4 :

The only change from the previous test case is taking a finer mesh, with 994 nodes (47 control variables). The two mesh are given in Figure 18 and 19 . Here, like in the test case 2, we are obliged to increase the accuracy of system resolution and, in spite of that, the convergence is rather slow; we can see on Figure 21 a comparison between the convergence history for the finer mesh and the precedent one (the computation is made here with the same number of Jacobi relaxation). On the solution presented in Figure 20 a high frequence appear in the first iteration and then disappears with difficulty; an explanation is that in our numerical scheme, the normal to boundary used for moment pressure fluxes is computed as the geometrical average of the normals to the two boundary edges of a boundary vertex; whether this problem would disappear if a cell-centered finite-volume scheme were applied is an open question.

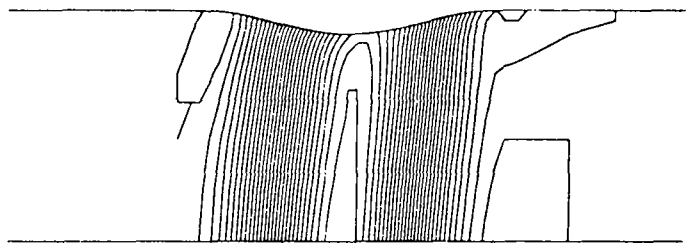

Figure 7: Shape γ_1 (Mach contour)

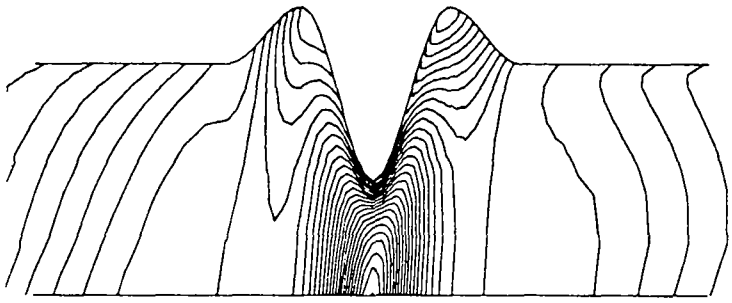

Figure 8: Shape γ_2 (Mach contour)

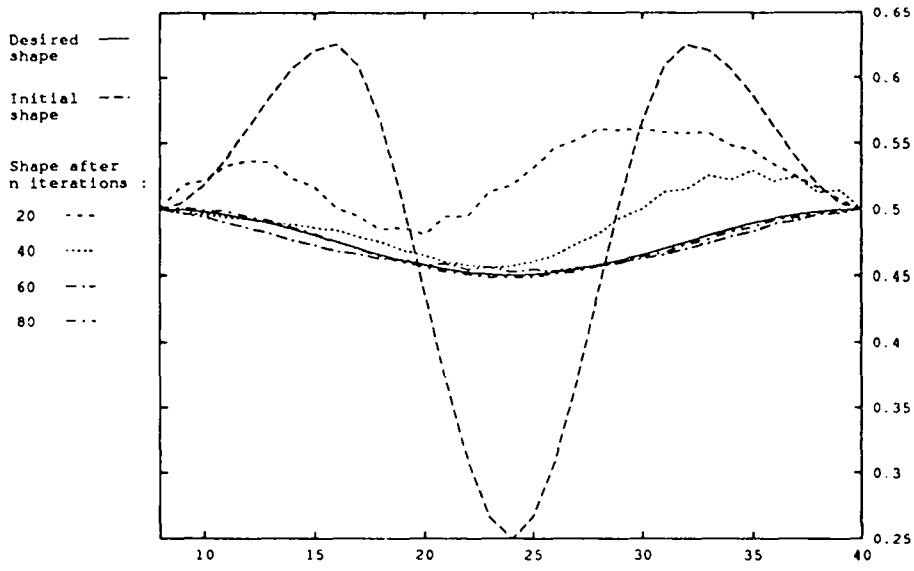

Figure 9: Test case 1 : Shape 40 iterations by 40 iterations

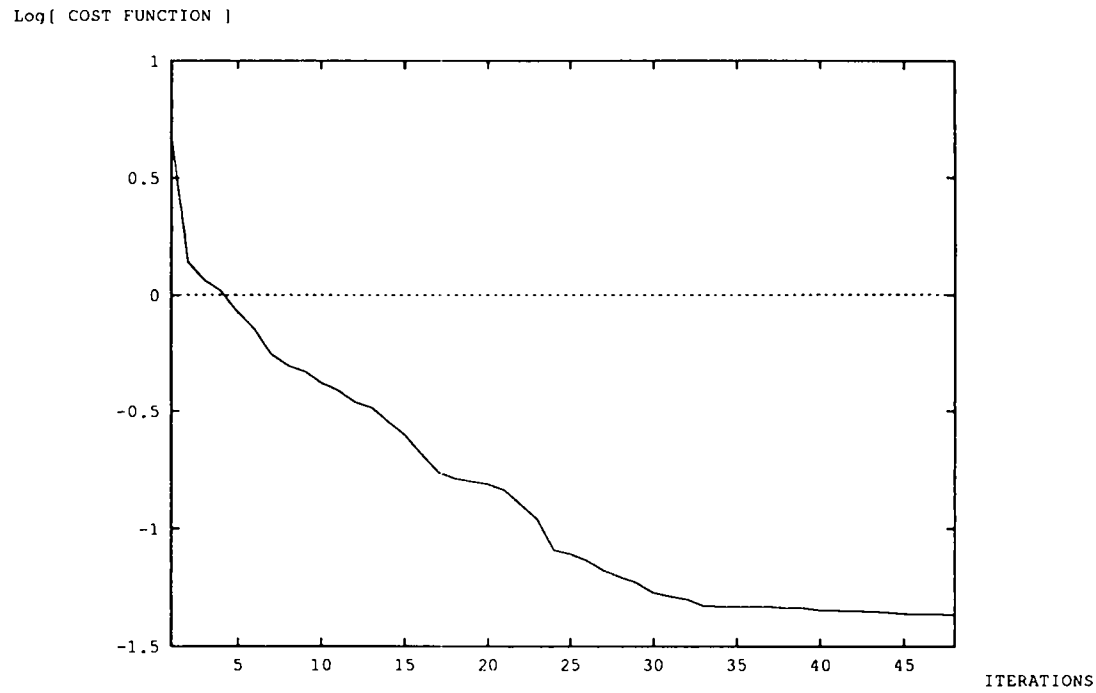

Figure 10: Test case 2 (few Jacobi relaxations): convergence history

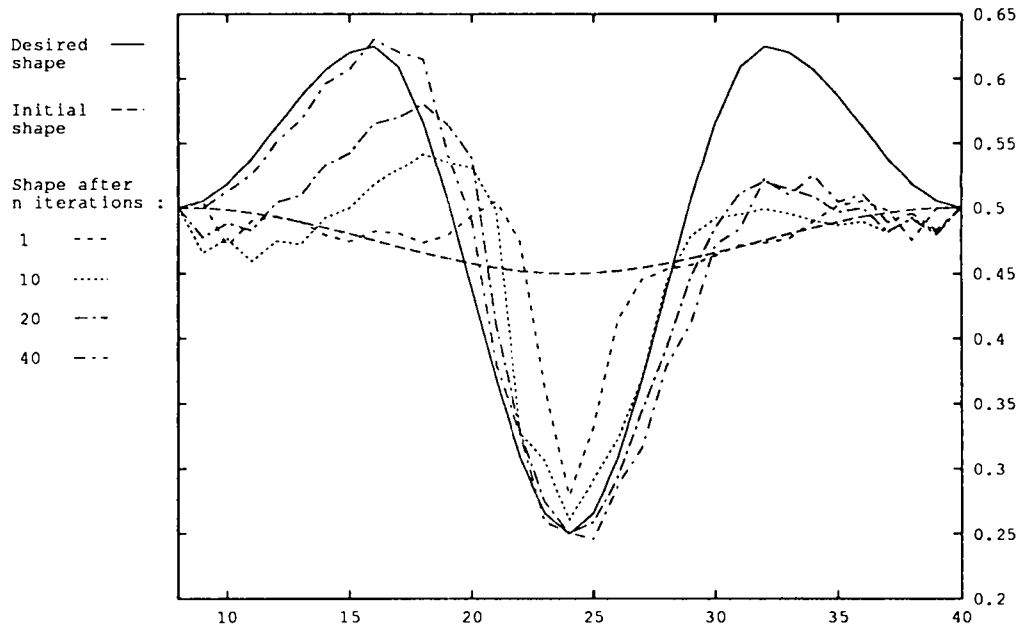

Figure 11: Test case 2 (few Jacobi relaxations): Successive shapes

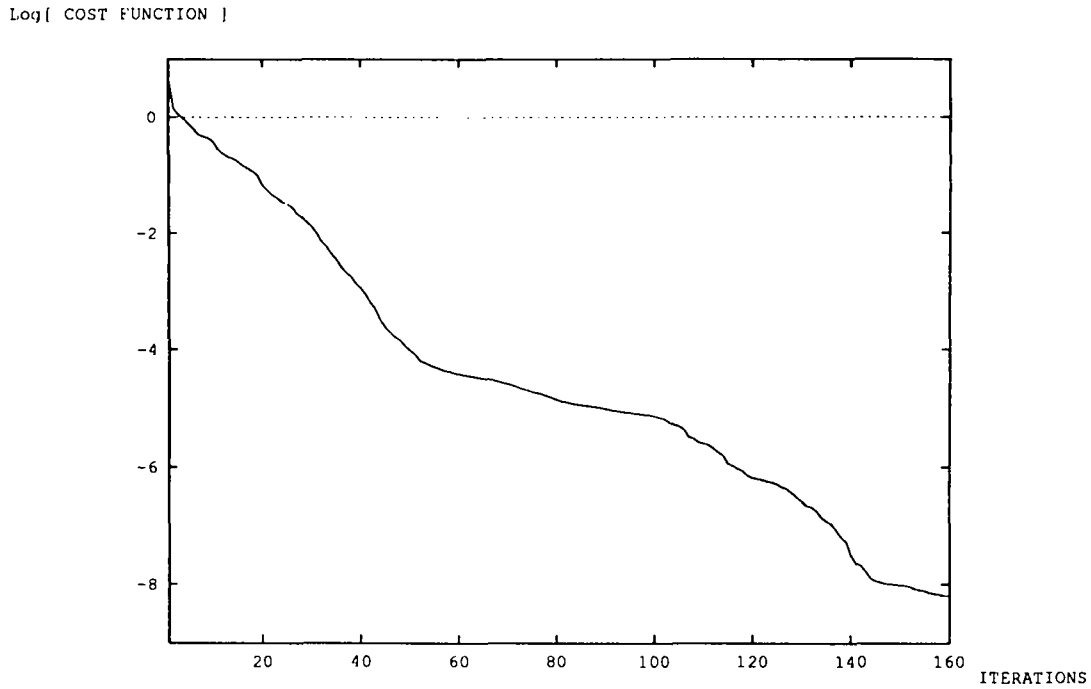

Figure 12: Test case 2 : convergence history

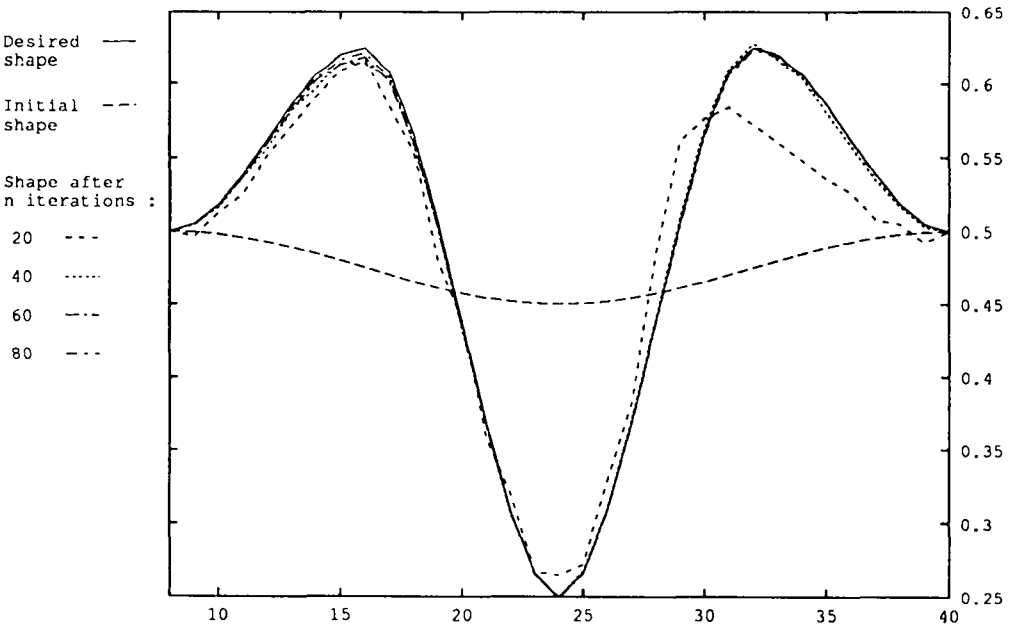

Figure 13: Test case 2 : Successive shapes

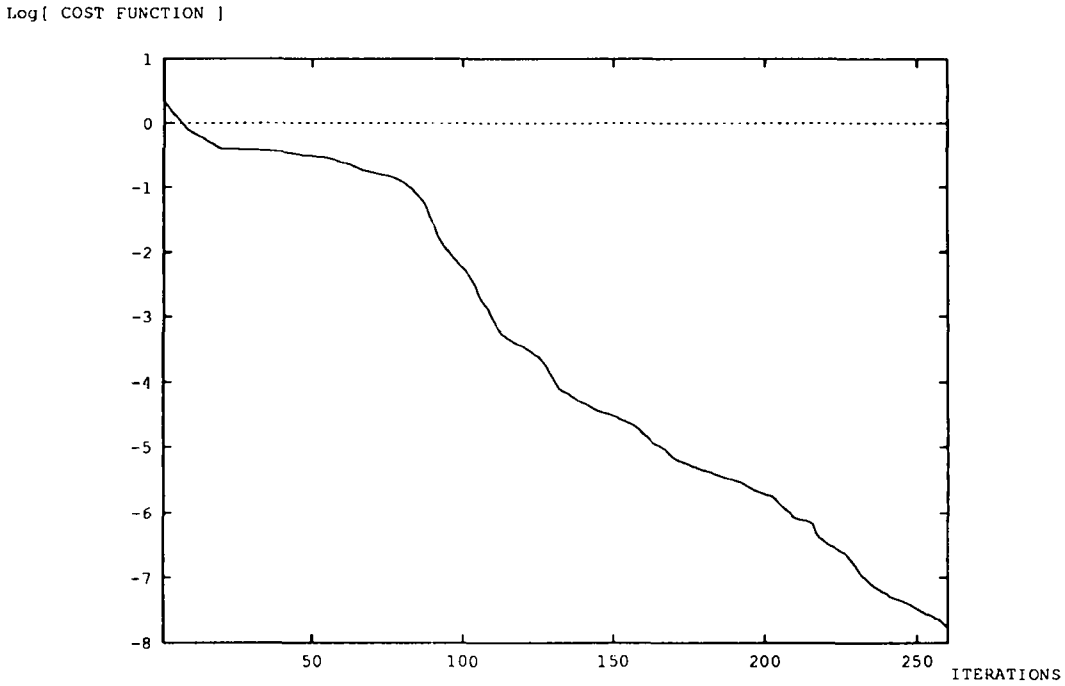

Figure 14: Test case 3 : convergence history

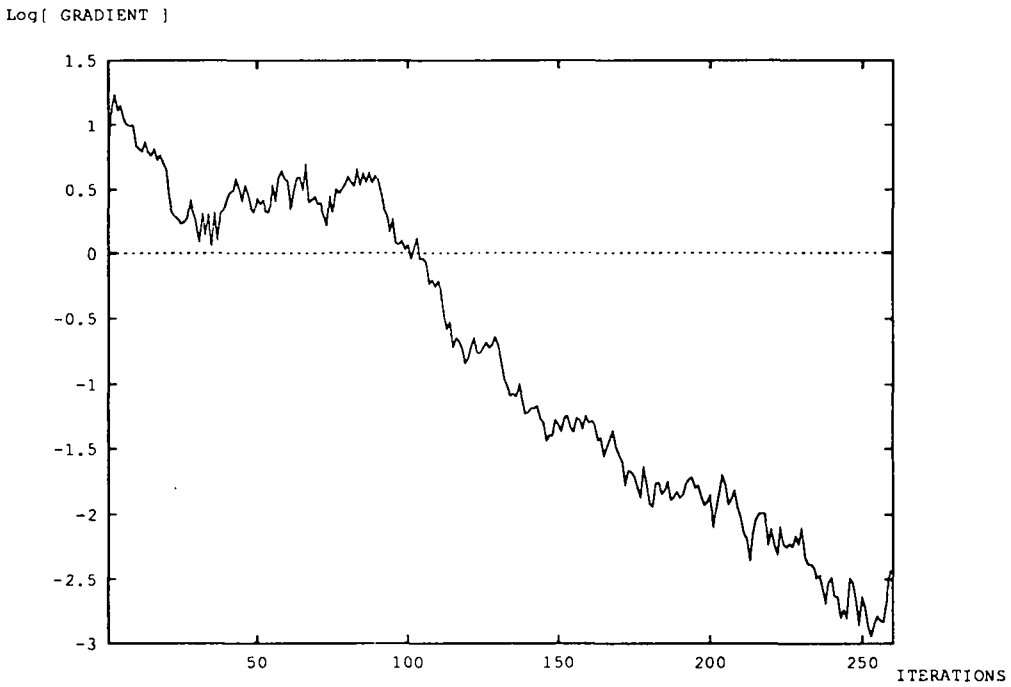

Figure 15: Test case 3 : Gradient

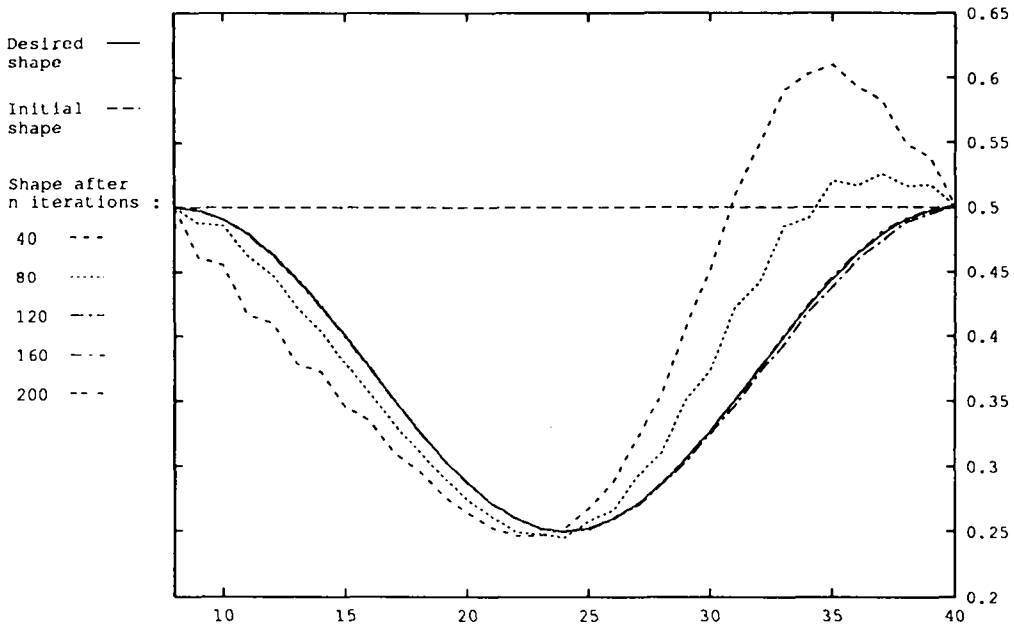

Figure 16: Test case 3 : Shape 40 iterations by 40 iterations

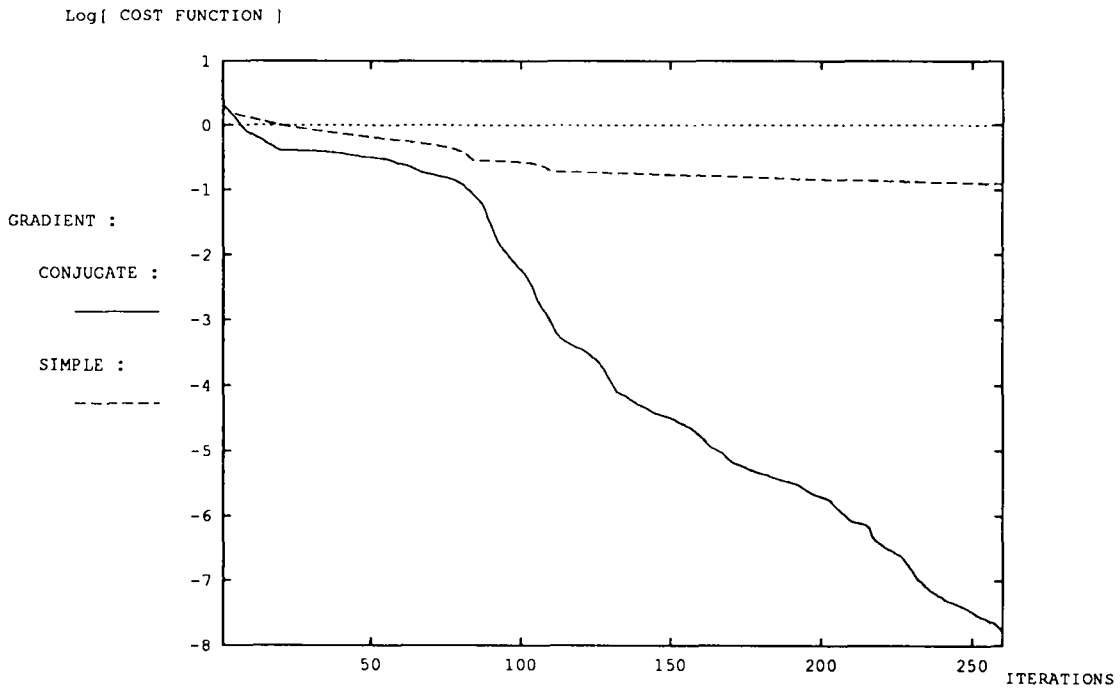

Figure 17: Test case 3: convergence history for simple and conjugate gradient

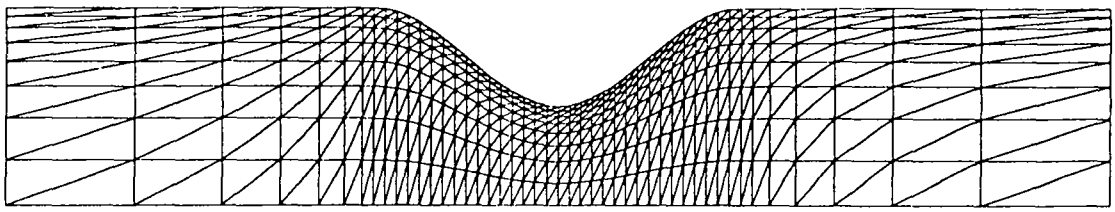

Figure 18: Mesh : 423-nodes

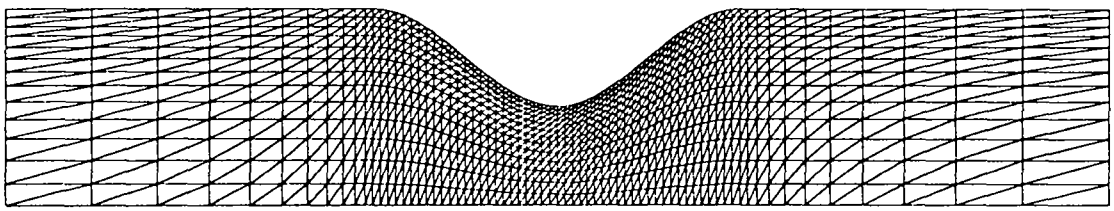

Figure 19: Mesh : 994-nodes

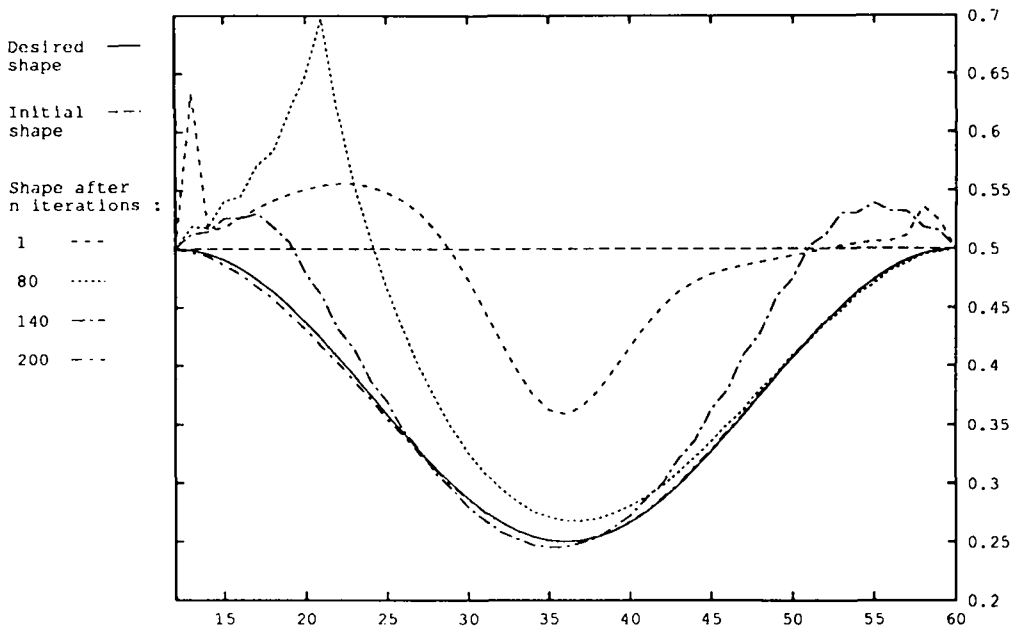

Figure 20: Test case 4 : Successives shapes

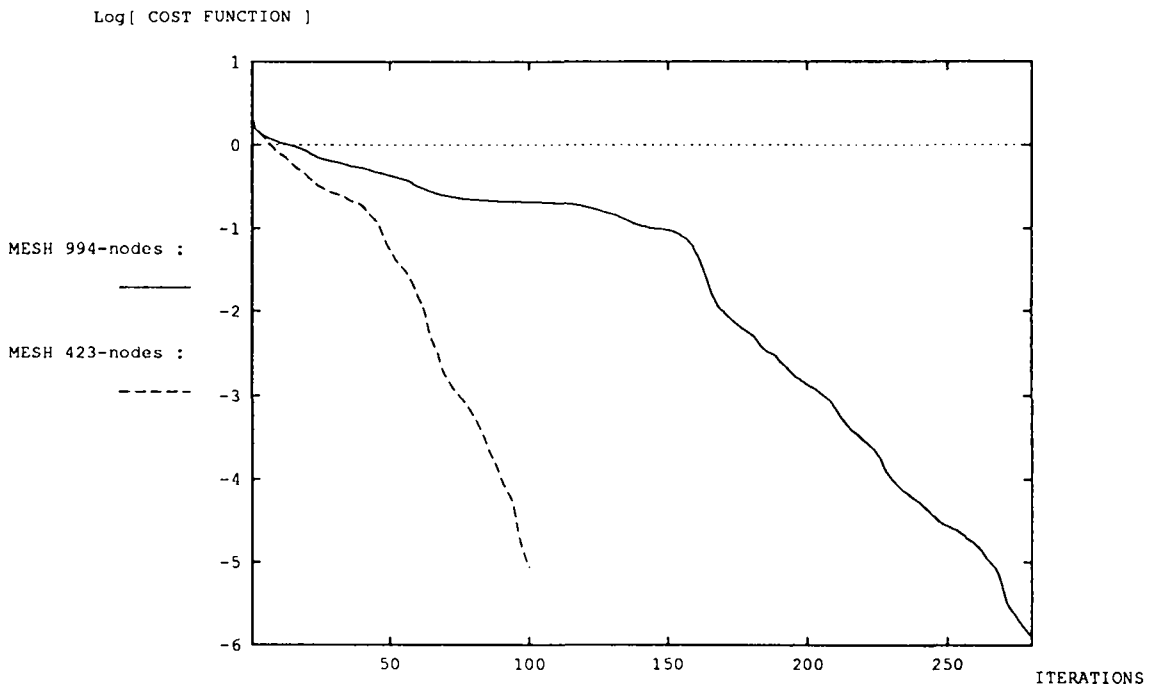

Figure 21: Test case 4 : convergence history

4.5 Some statistics

During all these calculations, the flow (direct system) was solved up to 4 decades in about 11 implicit time-iterations, each time-iteration involving about 20 linear Jacobi relaxations for test cases 1 and 3 and about 100 linear Jacobi relaxations for test cases 2 and 4. The adjoint system was solved by applying about the same accuracy as direct system. The rest of the optimization process, including computation of derivatives took less that 5 percent of the overall CPU cost, also when we use not many Jacobi relaxations.
On the finer mesh (for test case 4), one flow was computed in 70 seconds and one conjugate gradient iteration, involving about 4 cost evaluations took about 300 seconds on a SUN 4/40, without a complete vector optimization.

5 Concluding remarks

The smooth dependence of a mathematical flow model on the obstacle shape has been more or less intuitively recognized for many decades. We have exhibited formally its first variation with respect to the shape. We have also demonstrated that a numerical Euler model could be exactly differentiated with respect to the shape. In particular, with an upwind formulation, the adjoint state system is observed to be well-posed and easily solved by Jacobi relaxation.
We have presented several experiments for which the conjugate gradient method is a fully convergent (near double precision zero) optimization algorithm.
We have also described several cases for which the convergence is more difficult. It is then necessary to ensure that iterative solvers are enough converged, it is also clear that these problems are related to the rather non-smooth behaviour of the Euler system (singularity in solutions, non uniqueness when separation occurs). This non-smoothness can be further excited by the lower sensitivity of the numerical scheme chosen to high frequencies in the shape representation.
For less academical optimizations, it is necessary to update the present formulation to second-order spatial accuracy ; we think it is possible if a MUSCL formulation with smooth limiters is applied (see [8]); but doing this without an automated differentiator can be rather tedious.
Another critical point is the extension to non-structured mesh for handling complex geometries; it is in fact essentially done in our experimental computer program since most calculation are done element by element; only the mesh parametrization relies on the $i-j$ structure. We turn finally to the two main questions.
Firstly the present optimization process fails for many cases so that it can be used (without improvement) only for optimization with small variations of the shape; now it can be already useful in this restricted context.
Secondly, even when it works, convergence is still too expensive, since tens or hundreds flows are computed during the process. For both questions, we think that important improvements could be brought by the use of a set of adequate parametrizations of the shape, a topic that we are now investigating (see [11]) .

A Annex 1 : existence of a differentiable prolongation

We consider the parametrization (γ, Γ_{ad}) introduced in Section 2.1.

Lemma :

Let us assume that Γ_{ad} is a subset of $C^3(I\!R^2, I\!R^4)$ and let z_γ be the solution of the Dirichlet problem :

$$\begin{aligned} \Delta z_\gamma &= 1 \ \ on\ \Omega_\gamma \\ z_\gamma &= 0 \ \ on\ \partial\Omega_\gamma \end{aligned} \tag{12}$$

then there exists a differentiable application $\bar{z} : \Gamma_{ad} \rightarrow C^2(I\!R^2, I\!R)$ such that $\forall \gamma \in \Gamma_{ad}$, $\bar{z}(\gamma)|_{\Omega_\gamma} = z_\gamma$ solution of (12)

Sketch of proof (a detailed proof is given in [6]) :

In a first step, we introduce a mapping M_γ from Ω_γ onto a fixed regular domain Ω of $\mathbf{R}^2$; then system (12) can be mapped onto Ω and its solution $\tilde{z}(\gamma) = z_\gamma \, o \, M_\gamma^{-1}$ is a differentiable application from Γ_{ad} to $C^m(I\!R^2, I\!R)$.
Then $\tilde{z}$ is extended to $I\!R^2$ by using a linear extension operator P (extension by reflections, cf for example [2]) ; then $\mathcal{P}\tilde{z}$ is again a differentiable application from Γ_{ad} to $C^m(I\!R^2, I\!R)$.

Finaly we consider :

$$\bar{z}(\gamma) = (\mathcal{P}\, z_\gamma \, o \, M_\gamma^{-1}) \, o \, M_\gamma \, ;$$

Then $\bar{z}$ fulfils (12) .

B Annex 2 : continuum mechanics lemmas

We express here classical and less classical derivative lemmas in Continuum Mechanics. The proofs are given in [4].

Let Θ a regular domain such that for all $\Omega_\gamma \quad \bar{\Omega}_\gamma \subset \Theta \subset I\!R^n$
and C a differentiable application : $\Theta \times C^l(\partial\Omega) \rightarrow C^2(\bar{\Theta})$ with $l \geq 1$.

Lemma 1:

$$\frac{d}{d\gamma}[\int_{\Omega_\gamma} C(\gamma)\, dx] \,.\, \delta\gamma = \int_{\Omega_\gamma} \frac{\partial C}{\partial \gamma}(\gamma) \,.\, \delta\gamma \, dx + \int_\gamma C(\gamma) < n, V > \delta\gamma \, d\sigma$$

Where n is the unitary outward normal vector on γ and
V a regular vector field (see Section 2.1, Figure 1).

Lemma 2:

$$\frac{d}{d\gamma}[\int_{\Omega_\gamma} C(\gamma)\, d\sigma] \,.\, \delta\gamma = \int_\gamma \frac{\partial C}{\partial \gamma} \,.\, \delta\gamma \, d\sigma + \int_\gamma < grad_x C, n > \; + H\, C \; < n, V > \; \delta\gamma \, d\sigma$$

Where H represents the curvature of γ

Using Lemma 1 and Green formula :

Lemma 3:

$\forall \varphi \in C^1(\bar{\Theta})$

$$\frac{d}{d\gamma}[\int_\gamma \varphi \frac{\partial C(\gamma)}{\partial n}\, d\sigma] \,.\, \delta\gamma = \int_\gamma \varphi \frac{\partial}{\partial n}[\frac{\partial C}{\partial \gamma} \,.\, \delta\gamma]\, d\sigma$$

$$+ \int_\gamma [< grad_x\, C, grad_x\, \varphi > \; + \varphi\, \Delta_x C] < n, V > \; \delta\gamma \, d\sigma$$

C Annex 3 : a pseudo second order accuracy

Updating our first-order spatial accurate approximation to a second order formulation might be a rather tedious task; we can consider, first, an other alternative; i.e. use a mixed formulation, doing a second-order computation for the solution of Euler equations and a first-order calculation for the different derivatives and the adjoint state.
For the test case 3, we have compared at the first iteration, the first order gradient (obtained by differences divided and by adjoint method), the second order divided differences gradient and the gradient obtained with the precedent method. For the divided finite differences, we have choose the optimum value found in the Section 4.2 ($\varepsilon = 10^{-8}$), we can see on the following figure the differents gradients in function of the abscissa.

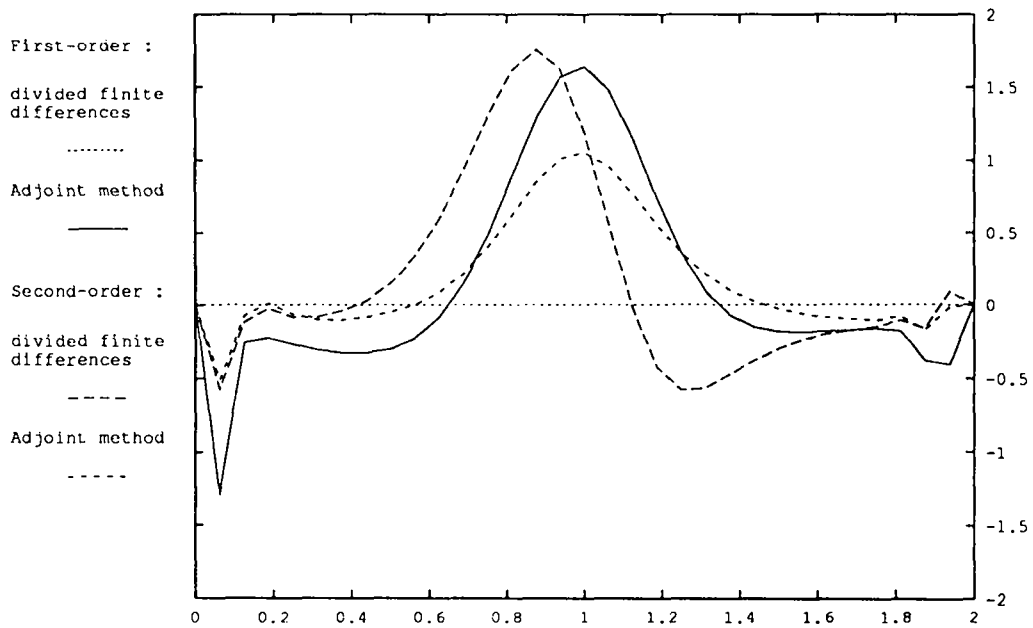

Figure 22: Comparison between the different gradients

We can notice first that we cannot distinguish the two first-order gradient but the pseudo second-order gradient is quite different from the second-order divided differences and not better than the first-order one; it might be even more clever to use the fully first-order gradient for a second-order optimization.

Acknowledgements

This programme was supported by Brite Euram 1082 Contract (Optimum Design in Aerodynamics) . We thank our colleagues L. Fezoui and H. Steve for yielding their implicit Euler finite-element code .

References

[1] J. HADAMARD *"Mémoires sur le problème d'analyse relatif à l'équilibre des plaques élastiques encastrées (1908) "*, œuvre de Jacques Hadamard, C.N.R.S., Paris, 1968

[2] J.L. LIONS *"Problèmes aux limites dans les équations aux dérivées partielles"*, Les Presses de l'Université de Montréal (1962)

[3] B. PALMERIO , A. DERVIEUX *"Une formule de Hadamard dans des problèmes d'identification de domaines"*,C.R Acad. Sci. Paris Série A , 1975

[4] F. MURAT , J. SIMON *" Sur le contrôle par un domaine géométrique"*, Laboratoire d'Analyse Numérique, Université Paris VI, 1976

[5] M.O. BRISTEAU *" Application of a Finite Element Method to Transonic Flow Problems using an Optimal Control Approach "*, Von Karman Institute for Fluid Dynamics Rhodes-Saint-Genèse (Belgium), Lecture Series 1978 - 4

[6] A. DERVIEUX *"Perturbation des équations d'équilibre d'un plasma confiné : comportement de la frontière libre, étude des branches de solutions"*, Rapport de Recherche INRIA No 18 , Mai 1980

[7] J. CEA *" Numerical Methods of Shape Optimal Design"*, Optimization of Distributed Parameter Structures (Eds E.J. Haug and J. Cea) Sijthoff & Noordhoff, Alphen aan den Rijn, Netherlands, 1981

[8] L. FEZOUI , B. STOUFFLET *"A class of implicit upwind schemes for Euler simulations with unstructured meshes"*, INRIA Research Report No 517 , April 1986

[9] A. JAMESON *" Aerodynamic design via control theory. "*, Report 1824 MAE, Princeton University (USA), May 1988

[10] O. PIRONNEAU A. VOSSINIS *"Comparison of some optimization algorithms for optimum shape design in aerodynamics "*, INRIA Research Report No 1392 , February 1991

[11] F. BEUX A. DERVIEUX *"Hierarchical shape optimization"*, In preparation

Imprimé en France
par
.l'Institut National de Recherche en Informatique et en Automatique.

ISSN 0249-6399